Object-based crop classification using multitemporal OLI imagery and Chain Classification with Random Forest

Bruno Schultz [1,2]
Markus Immitzer [2]
Antônio Roberto Formaggio [1]
Clement Atzberger [2]

[1] Instituto Nacional de Pesquisas Espaciais - INPE
Caixa Postal 515 - 12227-010 - São José dos Campos - SP, Brasil
{schultz, formagg}@dsr.inpe.br

[1] Institute of Surveying, Remote Sensing and Land Information,
University of Natural Resources and Life Sciences (BOKU), 1190 Vienna, Austria
{markus.immitzer, clement.atzberger}@boku.ac.at

Abstract. The use of more than one Landsat-like data sensor to automatically classify different crops is still a challenge. Improvements have been made using different images to map crops for large areas. The chain classification (CC) has permitted the use of samples in the overlapping area (between two Landsat-like images) to classify cultures at regional scale with an automatic classification. The Random Forest (RF) model is an automatic ensemble learning classifier with possible feature selection. RF can also provide reliability measures of the classification results for each segment. The goal of this work was to analyze the sugarcane classification in South of São Paulo State, using object-based approach, multitemporal images, random forest and chain classification. In the first step the images from August/2013 and January/2014 (221/76 and 222/76) were segmented and reference samples were manually selected from MCC (medium cycle crop), SCC (short cycle crop), LCC (long cycle crop), Water body (WB) and others (OT) to generate the first RF model (M1=overlapping). In the Second step we extracted the samples with high majority difference from the RFM1 model. After that, the best samples were used to classify each image in the second model (M2=221/76) and third model (M3=222/76). The obtained overall accuracies (OA) were 77.2 % (221/76) and 73.4 % (222/76). The results could may be improved if the samples were selected from low and high majority difference values.

Key words: chain classification, random forest, multitemporal image analyzis, objects based image classifcation.

1. Introduction

The Landsat satellite family is the most common program that is used to evaluate temporal changes in the land cover. The application of this data permits an improved management in terms of economy, environment, public health, human well-being and national security (Roy et al. 2014). Benefits from these data are estimated to amount to 935 million dollars per year (Miller et al. 2013). Much of this benefit is related to crop monitoring.

Even with the availability of Landsat data since 1972, Brazil still does not have a capable system for acreage and yield estimation of main crops with remote sensing (RS) images (Becker-Reshef et al. 2010; Atzberger 2013). The main limitation disfavoring crop classification and monitoring in tropical countries, is the clouds interference (Sugawara et al. 2008; Sano et al. 2007). However, today there is a large quantity of data from different types of Landsat-like sensors, which can be used jointly for developments of RS approaches for the Brazilian agriculture.

The open question remains on how all these RS data can be integrated in large scale monitoring, to reduce the amount of clouds in targeted areas? The summer crops in Brazil have a short cycle (3-4 months) and the Landsat-like images have a high revisit frequency (Powell et al. 2007). Each image in a mosaic must have an adequate amount of training data for classification and validation (Cihlar 2000; Pax-Lenney et al. 2001; Knorn et al. 2009).

This seems economically inviable for a country like Brazil, which has agricultural areas distributed nationwide. The alternative has been to use of overlapping area between images for training and classification of neighboring images (Knorn et al. 2009).

To avoid the application of the regression equations (Cihlar 2000) or the utilization of space-time signature extensions (Pax-Lenney et al. 2001), Knorn et al. (2009) have used the overlapping area (across and along-track) between images in chain, without atmospheric correction of the images. This methodology has become known as “Chain Classification” (CC). Its main goal is the utilization of overlaps between RS images to train and classify neighboring images, thus reducing the necessary amount of field/reference samples.

Many automatic classifiers of RS images can be used in CC technique, however the Random Forest (RF) algorithm is one of the newest and has shown good accuracy results to classify different land uses and covers (Ghimire et al. 2010; Immitzer et al. 2012), and separating crops with RS images (Rodriguez-Galiano et al. 2012; Long et al. 2013; Pal 2007). The multitemporal analysis of images (MA) and object based approach (OBIA) are further approaches which can improve the final mapping quality with RF. The use of OBIA in agriculture has promoted the image segmentation in objects look like crop productive units (PUs), and the images used in MA follow the UPs’s phenological phases at the time (Yan and Roy, 2014; Vieira et al., 2012). These two approaches applied together have obtained Kappa Indices higher than 0.75 in crop classification with decision tree (DT) algorithm (Peña-Barragán et al. 2011; Vieira et al. 2012)

The objective of this study is to determine the quantitative error of RF automatic classification for sugarcane mapping (medium cycle crop) by using chain classification with two (multitemporal) Landsat images.

2. Work´s Methodology

2.1 Study area and orbital images

The study area is located between the southern part of São Paulo State and the extreme north of Paraná State (Figure 1.a). This area can be characterized by planting soybean and “safrinha” corn (IBGE, 2012). Besides, the cultures of sugarcane, cassava, peanut, coffee, citrus, silviculture are parts of these municipalities agricultural chain. Even if the sugarcane fields have been located in the North of São Paulo State (Rudorff et al. 2010), the Figure 1.b shows that the sugarcane PUs also cover areas in the Assis-SP, Bauru-SP, Presidente Prudente-SP, Norte Central Paranaense-PR and Norte Pioneiro-PR mesoregions.

In this location the Operator Land Imager (OLI) images, from path/row 221/76 and 222/76, have been found (Figure 1.c and Figure 1.d). OLI sensor bands Blue (430 – 450 nm), Green (450 – 520 nm), Red (530 – 590 nm), Nir (850 – 880 nm), Sw1 (1.570 - 1.650 nm) and Sw2 (2.110 - 2.290 nm), from the months of August/2013 and January/2014 were used. The images were taken on the first OLI pass in August and the second pass in January.

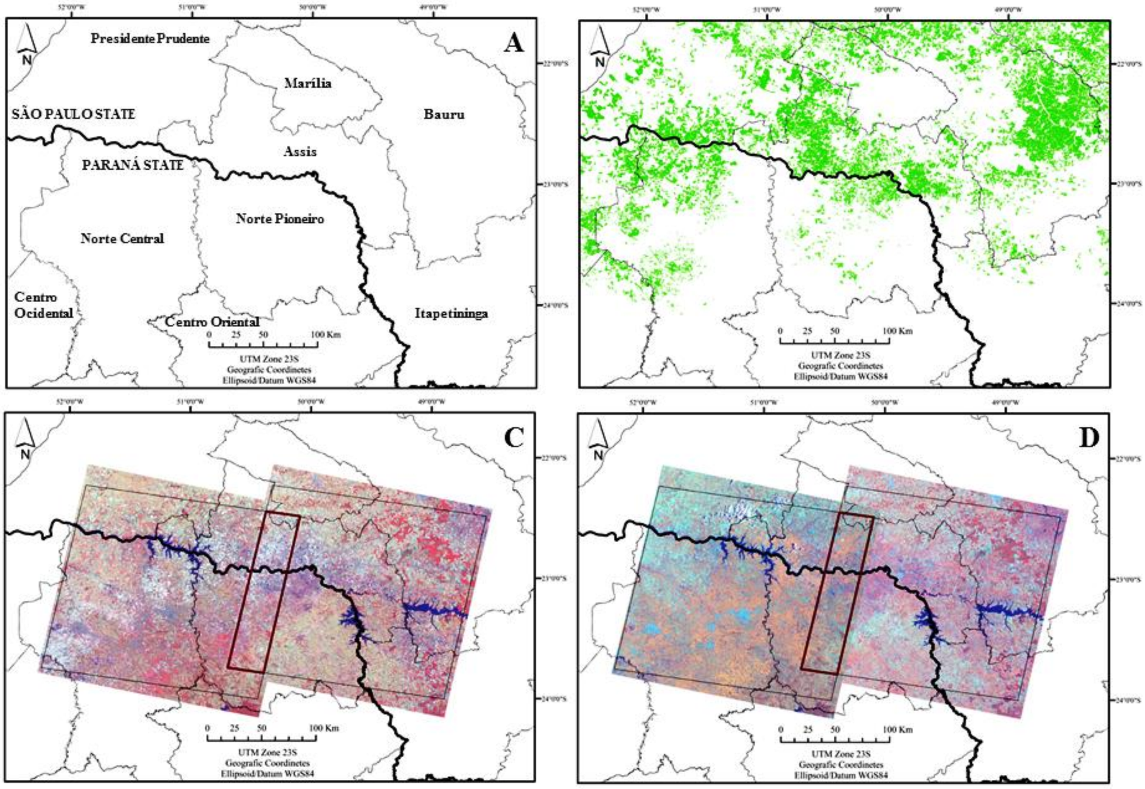

Figure 1. Study area. **(A)** State and mesoregions boundaries, **(B)** Sugarcane area 2011/2012, **(C)** OLI image (5)R (6)G (4)B August 2013 (DOY 233 and 242) and **(D)** OLI image (5)R (6)G (4)B January 2014 (DOY 028 and 037).

2.2 Training data set

The work field was carried out on images of January (28th January/2014 and 4th February/2014), 663 pixels located in the Assis mesoregion were selected by stratified random sampling. This Mesoregion is composed of 2 microregions (Assis and Ourinhos), and the Assis microregion is located in the overlap area from Landsat path 222 and 221. Between 7th to 12th of march 52 reference points (x,y) in this overlap area were carried out, belonging to the pre-defined sample frame from mesoregion area.

The reference was performed considering the lag-time between images and field work The labeled class was the present one at the time of sensor passed the study area. In field work the spectral similarity among peanut, cassava and soybean (short cycle crops) was noticeable. Thus information about latitude/longitude of more 87 further pixels belonging to this three classes were collected. In total 139 pixel were collected represent cycle long crop (CLC) = silviculture and native forest (34), medium cycle crops (MCC) = sugarcane (33), short cycle crop (SCC) = soybean, peanut and cassava (32), others (OT) = urban area, pastures, pre-planting area and sugarcane harvested (37) and water body (WB) (3). In the lab it was possible to select 929 objects which were similar to those found in field UPs, using OLI images from May/2013 until January/2014. The objects classification appurtenant of each culture was based on the approaches shown by Sanches et al. (2005) and Rudorff et al. (2010). In the total following reference samples were available: LCC (126), MCC (218), SCC (260), OT (272) and WB (59). These samples were used as training data set for RF model to classify the overlap area between the 222/221 paths images.

2.2 Multitemporal image analysis (MA) and object based approach (OBIA)

EL-Magd & Tanton (2003) have commented that MA improve crop classification. The accuracy could be increased by 6 to 9% compared to single image classification. The main advantage of this technique can be obtained, when the temporal images are placed in strategic form respecting the different phenological phases of the crops (Penã-Barragan et al., 2010; Vieira et al., 2012). Images from August/2013 and January/2014 were used (Figure 1.c and 1.d), because in these dates it was possible to separate *bisada* and not *bisada* sugarcane harvest and fallowing summer crop areas in in the images of August and green vegetation from summer crops and one-half-year year sugarcane in the images of January.

The principal components (PCs) and also the fraction of soil, shadow and vegetation from Unmixed Linear Model (ULM), were added to a database for each image. The ULM fractions were helpful to classify crops São Paulo State (Mello et al. 2010; Atzberger et al. 2014). The first PCs have generated the ULM and also attributes to each object. The texture attributes (Haralick) have shown good results to classify sugarcane in São Paulo State (Vieira et al., 2012), and so also texture attributes were included.

The DT algorithms showed good results in the crop automatic classification. DT algorithm can use a lot of attributes from objects to generate classification trees. That good performance has been related to image segmentation and the PUS shape (Peña-Barragan et al., 2010; Vieira et al., 2012; Yan e Roy 2014). In the OBIA approach the Multiresolution Segmentation (MS) algorithm has been used to delineate the RS images, using the pixels similarity group, through three radiometers image weights: scale factor (SF), shape (sh) and compactness (cp) (Baatz and Schäpe 2000).

These weights are different for each land use and satellite scene. In this paper, several combinations amount SF, Sh and cp have been tested, and best results have been obtained with SF (105), sh (0.50) and cp (0.30) were applied in the image segmentation, to classify soybean, sugarcane, peanut, cassava and others.

2.3 Random Forest (RF) model

The RF model is a DT supervised classifier which use out-of-bag (OOB) technique to create a training data set (Pal, 2005). It is also possible to select the best attributes to make the classifier model (Long et al., 2010; Rodriguez-Galiano et al., 2012). RF can provide an additional output to evaluate the reliability of the classification.

CC technic has used training samples from neighboring images to classify the overlap area of other images. After that it was possible to select the best samples based on the reliability values (<u>Step 1</u>) to create a new and bigger input dataset. This data was used to make new models for each neighboring image (<u>Step 2</u>).

2.4 Canasat_2012 upgrade map

The Canasat_2012 map, localized on 222/76 and 221/76 OLI images, refers 2011/2012 crop year, was upgraded to 2013/2014 crop year. The methodology to create the map was based on the study of Rudorff et al. (2010) using temporal OLI images from May/2013 until January/2014. The Canasat_2013 new map has been used to validate the final CC classification with RF model.

For the quantitative evaluation of the result the overall accuracy Index (OA) and Kappa Index (κ) (Foody 2002) were used. The confusion matrix was created by comparing the binary validation map with the classification results.

3 Results and discussion

The results were divided in several sublevels:

- First RF model or Step 1

- Second RF model or Step 2, and
- Validation of the final result.

In the first and second steps, the results from the feature selection and samples validation for just the overlapping area were explained. For these two steps the class WB, OT, LCC, SCC and LCC were used in the sample selection and validation. In (2) the final result about the classification area for two images was validated with sugarcane areas arising for the upgraded CANASAT_2012 dataset.

3.1 First and second Random Forest model – Step 1 and 2

Amount all the attributes used in the RF model, the Figure 2 shows the accuracy of RF increasing (up) when some variables were selected to make the out-of-bag samples and trees.

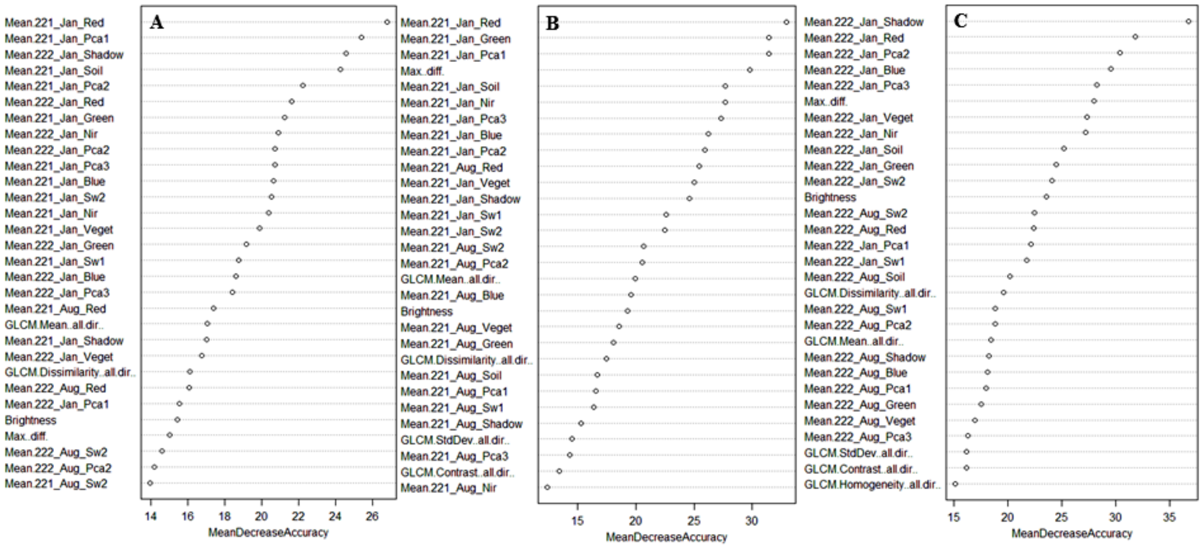

* Mean_222_Aug = DOY 233, Mean_221_Aug = DOY 242, Mean_222_Jaa = DOY 028, Mean_221_Jan = DOY 037

Figure 2. The top 30 variables in the OBIA and RF classification as ranked by order of importance. **(A)**. Variables used to make the sample RF model in step 1, **(B)**. Variables selected for the images from path 221 to make the RF model and in step 2 **(C)**. Variables selected for the images from path 222 to make another RF model in step 2

In the Figure 2(A) has been represented the importance of the two unmixed model fractions (Soil and Shadow) in January to separate the classes. Besides, the Red OLI band from January also was selected as a good variable. The Red band has been related with the greenness presents in the SCC objects. In January and February the soybean, peanut and cassava fields are in high vegetative vigor. The soybean and peanut canopy structures absorb the electromagnetic radiation in Red and the objects values get lower in this band (Sanches et al., 2005). The sugarcane canopy (MCC) structure favors the shadow increasing and the objects shadow values are higher than the SCC class.

For the Figure 2(B) and (C) the Max.diff. and GLCM Dissimilarity showed importance to separate the different crop classes. The Max.diff is an algorithm that computes the maximum and minimum mean value in the temporal image series (Stumpf and Kerle 2011). Image from August has showed SCC fallowing and some sugarcane areas in reform (i.e. low values of NIR). Between January and March, the fallowing areas are in green vegetation (i.e. high values in NIR) and the MCC have not the same spectral behavior as SCC (different canopy structures). The paths in the sugarcane fields also increase the soil spectral response, and the fast changes between the pixels favors the textural models (Vieira et al. 2012)

The validation of the three different models has been shown in the Table 1. The classification using OBIA, 4 images in multitemporal series (DOY 233/2013, 242/2013, 028/2014 and 037/2014) and RF model had high overall accuracy (OA = 95.91 %) in the overlapping are. Using images only from one path for classifying the overlapping area obtained OA of 95.69 % for 221/76 and 93.33 % for 222/76. Even the SCC be harvested faster than the MCC and LCC, the results between images were similar.

Table 1. Confusion matrices for the five classes evaluated in the overlapping area.

	RF model Step 1						RF model Step 2 image 221/76						RF model Step 2 image 222/76					
	OT	**BW**	**LCC**	**MCC**	**SCC**		**OT**	**BW**	**LCC**	**MCC**	**SCC**		**OT**	**BW**	**LCC**	**MCC**	**SCC**	
OT	**262**	0	0	3	0	265	**261**	0	0	4	0	265	**247**	0	0	12	6	265
BW	0	**59**	0	0	0	59	0	**59**	0	0	0	59	1	**58**	0	0	0	59
LCC	0	0	**121**	2	3	126	0	0	**122**	2	2	126	0	0	**120**	3	3	126
MCC	10	0	0	**200**	8	218	11	0	0	**200**	7	218	17	0	1	**193**	7	218
SCC	0	0	1	11	**249**	261	1	0	1	12	**247**	261	1	0	1	10	**249**	261
	272	59	122	216	260	929	273	59	123	218	256	929	266	58	122	218	265	929

OOB estimate of error rate: **4.09%** OOB estimate of error rate: **4.31%** OOB estimate of error rate: **6.67%**

After the models classify the overlapping area in each image, the result of the validation using the first quintile samples were 99.95% and 99.27% the image 221/76 and 222/76 respectively. The 25 % of the samples had the highest classification reliability. Due to the nine day difference in the images acquisition, the selection of reliability objects in RF model have not used areas of the same object with different spectral behaviors as samples (see 1, 2, 3 and 4 signs in the Figure 3). Figure 3 shows areas that could be selected as same crop if majority objects would be not used in chain classification approach.

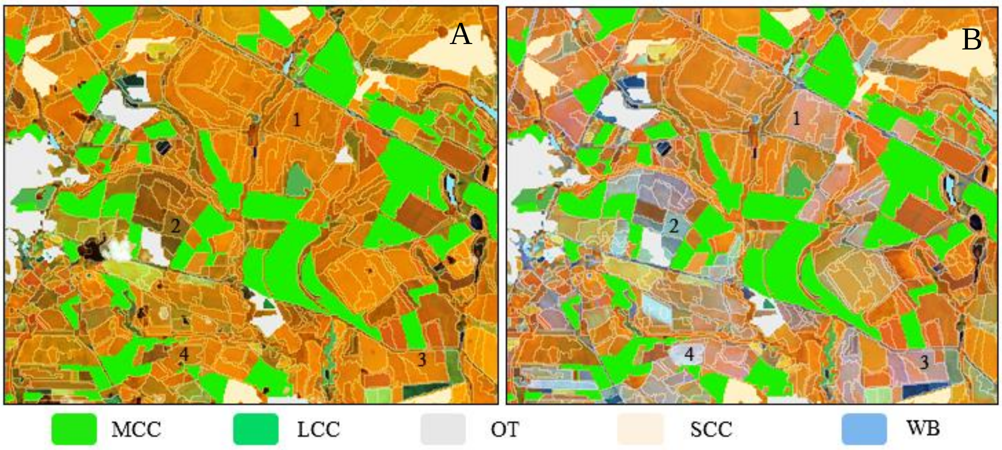

Figure 3. 25 % of the best samples for each class were selected for the reliability RF methodology. **(A)** Images from DOY 028/2014 and **(B)** Images from DOY 037/2014.

Knorn et al., (2009) have worked with SVM algorithm to classify forests (LCC) in chain classification (CC). LCC does not show the same rapid changes such as SLC and so the CC methodology provided good results creating a forest map. The overall accuracy (OA) in Knorn's work was between 92.1% and 98.9% (average of 96.3%). Even using five different classes to map in this work, the result was similar for each image (Table 1). The reliability sample information was useful to select the good automatic information samples for both images. The Step 1 has shown just results in cross-validation amount samples, and the Step 2 will show the result with the binary reference map information for all the area (two images).

3.2 Validation sugarcane (MCC) map

The OA classification results for each image were 77.2 % (221/76) and 73.4 % (222/76). These results could be improved if in step 2, also “bad samples” were used next to the “best samples” using the reliability information. Often the use of less unambiguous samples in the model leads to better results in the model application.

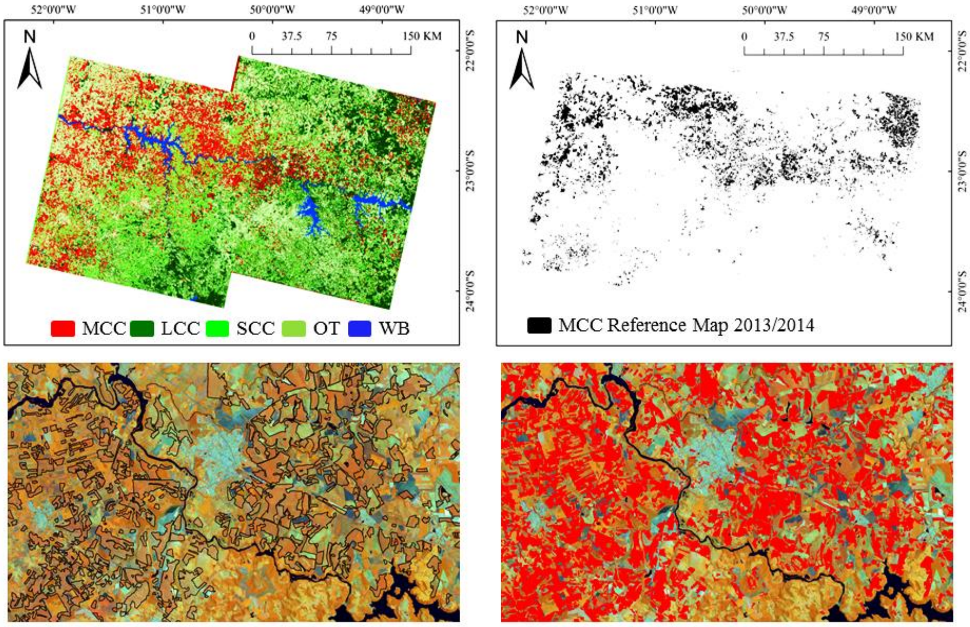

Reference Map 2013/2014 Chain classification with RF approach

Figure 4. Chain classification + RF approach classification results to MCC.

The selection only the first quartile in Step 2, kept automatically samples from the middle of the objects distribution and the distribution tales have been missed. Even being considered the best samples, the crops have not the same spectral behavior in all UP. Thus, it is necessary to select after the reliability information, new samples for each class but from different majority values.

4 Conclusions

- The obtained accuracy for MCC was satisfactory.
- The methodology could be tested in other Brazilian regions and for other crops.
- It is necessary to improve the sample selection method in Step 2.

Acknowledgments

We would like to thank the “Science without Borders” program for the PhD sandwich scholarship, the IFVL team from BOKU and as well MoBARS team from INPE.

Bibliographic References

Atzberger, C., 2013. Advances in Remote Sensing of Agriculture: Context Description, Existing Operational Monitoring Systems and Major Information Needs. *Remote Sensing*, 5(2), pp.949–981.

Atzberger, C. et al., 2014. Obtaining crop-specific time profiles of NDVI : the use of unmixing approaches for serving the continuity between SPOT-VGT and PROBA-V time series. *International Journal of Remote Sensing*, (July), pp.37–41.

Baatz, M. & Schäpe, A., 2000. Multiresolution Segmentation : an optimization approach for high quality multi-scale image segmentation. In *Angewandte Geographische Informationsverarbeitung XII*. pp. 12–23.

Becker-Reshef, I. et al., 2010. Monitoring Global Croplands with Coarse Resolution Earth Observations: The Global Agriculture Monitoring (GLAM) Project. *Remote Sensing*, 2(6), pp.1589–1609.

Cihlar, J., 2000. Land cover mapping of large areas from satellites: Status and research priorities. *International Journal of Remote Sensing*, 21(6-7), pp.1093–1114.

Cutler, D.R. et al., 2007. Random forests for classification in ecology. *Ecology*, 88(11), pp.2783–92.

EL-Magd, I.A. & Tanton, T.W., 2003. Improvements in land use mapping for irrigated agriculture from satellite sensor data using a multi-stage maximum likelihood classification. *International Journal of Remote Sensing*, 24(21), pp.4197–4206.

Foody, G.M., 2002. Status of land cover classification accuracy assessment. *Remote Sensing of Environment*, 80, pp.185–201.

Ghimire, B., Rogan, J. & Miller, J., 2010. Contextual land-cover classification: incorporating spatial dependence in land-cover classification models using random forests and the Getis statistic. *Remote Sensing Letters*, 1(1), pp.45–54.

Immitzer, M., Atzberger, C. & Koukal, T., 2012. Tree Species Classification with Random Forest Using Very High Spatial Resolution 8-Band WorldView-2 Satellite Data. *Remote Sensing*, 4, pp.2661–2693.

Knorn, J. et al., 2009. Remote Sensing of Environment Land cover mapping of large areas using chain classi fi cation of neighboring Landsat satellite images. *Remote Sensing of Environment*, 113(5), pp.957–964.

Long, J.A. et al., 2013. Object-oriented crop classification using multitemporal ETM + SLC-off imagery and random forest. *GIScience and Remote Senssing*, (August), pp.37–41.

Mello, M.P. et al., 2010. Automatic Classification of Sugarcane Harvest Using Spectral Linear Mixing Model. *Revista Brasileira de Cartografia*, 2(62), pp.181–188.

Miller, B.H.M. et al., 2013. *Users , Uses , and Value of Landsat Satellite Imagery — Results from the 2012 Survey of Users*,

Pal, M., 2007. Random forest classifier for remote sensing classification. *International Journal of Remote Sensing*, 26(1), pp.37–41.

Pax-lenney, M. et al., 2001. Forest mapping with a generalized classifier and Landsat TM data. *Remote Sensing of Environment*, 77, pp.241–250.

Powell, S.L. et al., 2007. Moderate resolution remote sensing alternatives: a review of Landsat-like sensors and their applications. *Journal of Applied Remote Sensing*, 1, p.012506.

Rodriguez-Galiano, V.F. et al., 2012. An assessment of the effectiveness of a random forest classifier for land-cover classification. *ISPRS Journal of Photogrammetry and Remote Sensing*, 67, pp.93–104.

Roy, D.P. et al., 2014. Remote Sensing of Environment Landsat-8 : Science and product vision for terrestrial global change research. *Remote Sensing of Environment*, 145, pp.154–172.

Rudorff, B.F.T. et al., 2010. Studies on the Rapid Expansion of Sugarcane for Ethanol Production in São Paulo State (Brazil) Using Landsat Data. *Remote Sensing*, 2(4), pp.1057–1076.

Sanches, I.D., Epiphanio, J.C.N. & Formaggio, A.R., 2005. Culturas Agrícolas em imagens multitemporais do satélite Landsat. *Agricultura de São Paulo*, 52(1), pp.83–96.

Sano, E.E. et al., 2007. Spatial and temporal probabilities of obtaining cloud-free Landsat images over the Brazilian tropical savanna. *International Journal of Remote Sensing*, 28(12), pp.2739–2752.

Stumpf, A. & Kerle, N., 2011. Remote Sensing of Environment Object-oriented mapping of landslides using Random Forests. *Remote Sensing of Environment*, 115(10), pp.2564–2577.

Sugawara, L.M., Friedrich, B. & Rudorff, T., 2008. Viabilidade de uso de imagens do Landsat em mapeamento de área cultivada com soja no Estado do Paraná. *Pesquisa Agropecuária Brasileira*, 43(12), pp.1777–1783.

Yan, L. & Roy, D.P., 2014. Automated crop field extraction from multi-temporal Web Enabled Landsat Data. *Remote Sensing of Environment*, 144, pp.42–64.